Applied Acoustics 74 (2013) 189–197

Contents lists available at SciVerse ScienceDirect

Applied Acoustics

journal homepage: www.elsevier.com/locate/apacoust

Acoustic performance of gabions noise barriers: Numerical and experimental approaches

F. Koussa [a,*], J. Defrance [a], P. Jean [a], P. Blanc-Benon [b]

[a] Centre Scientifique et Technique du Bâtiment, 24 rue Joseph Fourier, 38400 Saint Martin d'Hères, France
[b] LMFA, UMR CNRS 5509, Ecole centrale de Lyon, Université de Lyon, 69134 Ecully Cedex, France

ARTICLE INFO

Article history:
Received 26 September 2011
Received in revised form 23 July 2012
Accepted 24 July 2012
Available online 17 August 2012

Keywords:
Gabions noise barriers
Scale model measurements
In situ measurments
BEM
Insertion loss

ABSTRACT

This research work aims at evaluating the acoustic performance of conventional and low height gabions noise barriers. On one hand, in situ as well as scale model measurements at a scale of 1:10 have been carried out to assess the intrinsic acoustic properties of a 3 m high gabions barrier. Single number ratings of transmission and reflection indices reached 20 dB and 5 dB, respectively. On the other hand, numerical simulations using a 2D boundary element method (BEM) and scale model measurements are carried out to study the effectiveness of low height gabions noise barriers when they are inserted in dense urban areas. The agreement between numerical and scale model measurements results is satisfactory. The effectiveness of low height gabions noise barriers is significant for receivers of limited height and the insertion loss values can reach 8 dB(A) behind the barrier. This confirms that gabions noise barriers are possible candidates as useful devices for environmental noise reduction.

1. Introduction

The negative effects resulting from exposure to road traffic noise are well-known. Barriers are now in common use as a solution for abating traffic noise. A large amount of research work has been carried out aiming at predicting their performance and developing more efficient designs. With respect to conventional roadside barriers, new acoustic barriers are essentially based on two basic principles: either applying sound absorbing materials or using new barrier shapes to modify the diffracting-edge. Gabions are boxes, made of twisted or welded steel wire, filled with stones that are used in civil engineering and road building applications. They are originally dedicated to the achievement of retaining structures or hydraulic protections. In this research, an idea is to use these natural gabions as noise barriers in urban areas. The intrinsic characteristics are relevant to qualify the noise barrier itself. They can be tested both outdoors and in laboratory. In this paper, we have performed in situ tests to determine the characteristics of sound reflection and transmission of gabions noise barriers in actual use according to the European CEN/TS 1793-5:2003 standard [1]. These normalized methods proved to be easy to use and reliable for most kinds of barriers. In the same context, another original idea of this research is to propose a third method to evaluate the intrinsic properties of gabions noise barriers by performing scale model measurements based on the same standards. In dense urban areas it is usually difficult to protect pedestrians and cyclists in the vicinity of road infrastructures without using devices that are too imposing. Therefore another objective in this work is to study the effectiveness of low height gabions noise barriers. These natural low height barriers have not been studied in the literature. However, a few studies have been carried out on conventional low height noise barriers (rigid, absorbent). For example, Anai and Fujimoto [2] showed that the insertion of a small noise barrier with a height that does not exceed 1 m can reduce the noise level by around 5 dB(A) behind the protection. Baulac et al. [3,4] studied the performance of low height noise barriers of different shapes and covered with an absorbent layer. The authors showed that the global effectiveness of such low height protections reaches 6–10 dB(A) behind the protection for pedestrian receivers. Thorsson [5] used an equivalent source method to optimize the performance of 1 m height noise protection. He found an optimum impedance boundary condition at the barrier surface and the results showed an improvement of 5 dB(A) in a configuration with an absorptive 1 m high barrier compared with a rigid barrier. Ding et al. [6] showed that low height porous barriers can improve the acoustic effectiveness up to 2 dB(A) when compared to geometrically identical rigid noise protection. In this case, the flow resistivity of the porous medium was shown to be an important parameter. Finally, Martin and Hothersall [7] studied the effect of the addition of a central reservation barrier between the road lines. They found an improvement of 1–2 dB(A) by the addition of such noise barriers. In this research, both numerical simulations using the boundary element method and scale model measurements

* Corresponding author.
E-mail address: faouzi.koussa@cstb.fr (F. Koussa).

0003-682X/$ - see front matter © 2012 Elsevier Ltd. All rights reserved.
http://dx.doi.org/10.1016/j.apacoust.2012.07.009

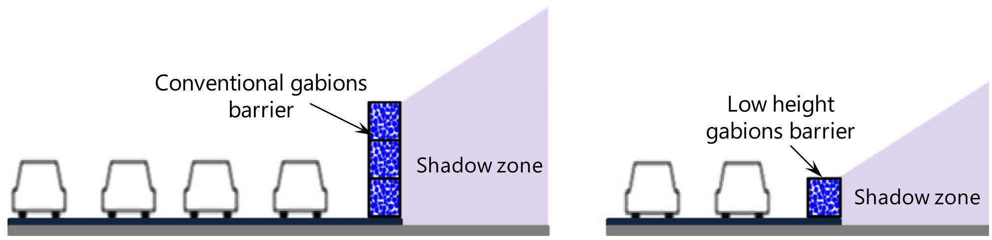

Fig. 1. Overall concept of conventional and low height gabions noise barriers.

are carried out to evaluate the effectiveness of low height gabions barriers in reducing the impact of road traffic noise. The concept of conventional and low height gabions noise barriers studied in this research is presented in Fig. 1.

The aim of this research paper is to evaluate the acoustic performance of gabions noise barriers using both measurements and BEM numerical simulations. In Section 2, in situ and scale model measurements of reflection and transmission properties of conventional gabions barriers are presented with a short description of the experimental set up; results and comparisons between the two experimental approaches are then discussed. Section 3 is devoted to low height gabions noise barriers. The numerical approach using the boundary element method is briefly described and convergence properties are discussed, numerical results for realistic multi-lane traffic noise situations are presented and compared with results from scale model experiments.

2. Experimental assessment of conventional gabions noise barriers

This section is divided into two parts: first, we present the CEN/TS 1793-5:2003 standard [1] in which the reflection and transmission indices are used to evaluate the acoustical intrinsic properties of gabions noise barriers. Then the experimental set up as well as the measurement method for both in situ and scale model measurements are detailed. In the second part, the results of the two experimental approaches are presented and compared.

2.1. Application of the CEN/TS 1793-5:2003 standard

2.1.1. In situ measurements

The aim of this section is to determine the in situ intrinsic characteristics of sound reflection and transmission of gabions noise barrier in actual use according to the CEN/TS 1793-5:2003 standard. Tests on a gabions noise barrier filled with crushed stones have been performed in Livet et Gavet (Rhône-Alpes, France) (Fig. 2). The height h_b, the width w_b, and the porosity ϕ of the gabions barrier are 3 m, 1.1 m and 0.4, respectively. The granulometry of the stones is 7/15 cm. It has been measured using a gradation test with a nested column of sieves of different screen openings.

We use the Adrienne test method already presented in several publications [8–10]. An impulsive method is used for the measurements with a JBL 2123H electro-acoustic source. The test signal is a MLS sequence of order 16 and 16 averages are performed for each impulse response acquisition with a sample rate of 44,100 Hz. The acquisition is achieved with a Pulse system developed by Brüel&kJær. All measurements have been carried out the same day within a period of 2 h. It was a sunny clear day with no significant wind. We considered therefore that the atmospheric conditions were the same all along the experiment period.

The Reflection Index (RI) and the Sound Insulation Index (SI) are introduced by the CEN/TS 1793-5:2003 standard respectively giving global indications on sound absorption and sound transmission properties of the noise barrier.

2.1.1.1. Reflection index. The measuring equipment located in front of the noise barrier consists of a sound source and a connected half-inch Brüel&kJær 4133 microphone. The source height is $h_s = h_b/2 = 1.5$ m and the source–receiver distance is 1.25 m. The microphone situated at 0.25 m from the noise barrier in normal incidence, receives a signal giving an overall impulse response. Measurements at nine different angles, between $-40°$ and $40°$ in steps of 10°, in front of the barrier are prescribed to evaluate normal and oblique incidence performances (Fig. 2). Each overall impulse response includes the direct component, travelling from the source to the barrier, the component reflected by the barrier and another parasitic component reflected from the ground: the first two components are separated using the signal subtraction technique while the third one should be cancelled out by time windowing. The signal subtraction technique consists in extracting the reflected component from the overall impulse response after having removed the direct component by subtraction of an identical

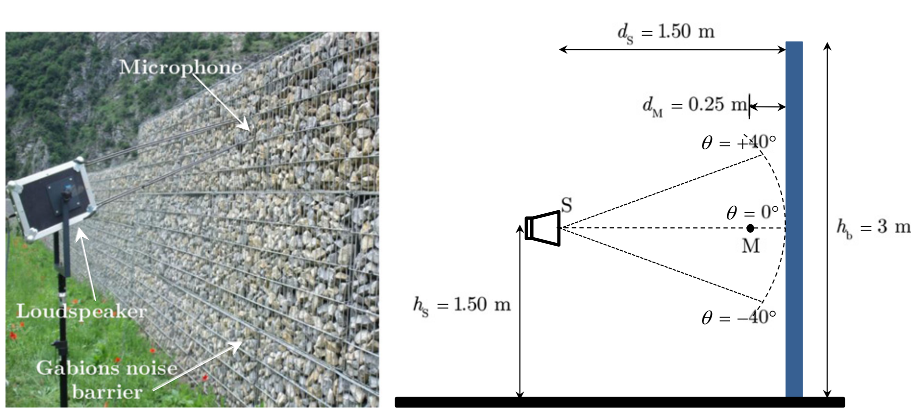

Fig. 2. Experimental set up for the in situ measurement of the reflection index of the gabions noise barrier.

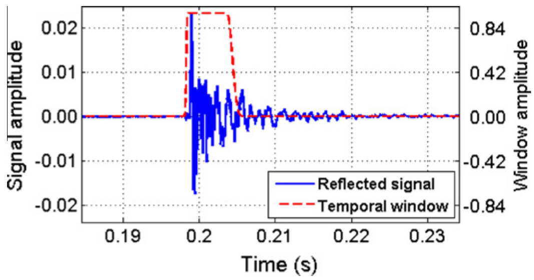

Fig. 3. Reflected component of the impulse response (solid line) for normal incidence and temporal window (dashed line).

signal. The last one is the free field signal measured using the same geometrical configuration of the loudspeaker and the microphone avoiding to face any nearby surface. The reflection index RI_j as a function of frequency, in one-third octave bands Δf_j, is computed using the following expression:

$$RI_j = \frac{1}{n_j}\sum_{k=1}^{n_j} \frac{\int_{\Delta f_j} |FFT[t \times h_{r,k}(t) \times w_r(t)]|^2 df}{\int_{\Delta f_j} |FFT[t \times h_i(t) \times w_i(t)]|^2 df} \quad (1)$$

In this formula, j is the index of the one-third octave band and $n_j \leqslant 9$ is the number of angles of measurement, $h_{r,k}(t)$ and $h_i(t)$ are the reflected component at the kth angle and the incident component of the free-field impulse response, respectively. $w_r(t)$ and $w_i(t)$ are the reflected component time window and the incident reference free-field component time window, respectively. t is the time whose origin is at the beginning of the impulse response acquired by the measurement chain. It takes into account the attenuation of the amplitude of the reflected component in a manner inversely proportional to the travel time. The single-number rating of sound reflection DL_{RI}, in decibels, is given by the following equation:

$$DL_{RI} = -10\log_{10}\left(\frac{\sum_{j=m}^{18} RI_j \times 10^{0.1L_j}}{\sum_{j=m}^{18} 10^{0.1L_j}}\right) \quad (2)$$

where L_j is the relative A-weighted sound pressure level (dB) of the normalized traffic noise spectrum, as defined in the European standard EN 1793-3:1997 [11], in the jth one-third octave band. m is the index of the low third octave band limit. An example of the impulse response of the reflected component after substraction of the incident signal at normal incidence and the Adrienne temporal window are given in Fig. 3.

2.1.1.2. Sound insulation index. The same equipment described above is used to evaluate the properties in transmission of the gabion noise barrier. The source–barrier distance is 1 m. The acoustic impulse response is recorded by a microphone which is placed in a grid of nine scanning points situated at 0.25 m behind the barrier (Fig. 4). It includes the transmitted component, travelling from the sound source through the gabions barrier and the component diffracted by the top edge of the gabions barrier. The last one is cancelled out by time windowing. The direct free-field wave is obtained when the measurement is repeated without the gabions barrier between the sound source and the microphone. The sound insulation index SI_j as a function of frequency, in one-third octave bands Δf_j, is the logarithmic average of the results in the nine scanning positions. It is computed using the following expression:

$$SI_j = -10\log_{10}\left(\frac{\sum_{k=1}^{n_j} \int_{\Delta f_j} |FFT[h_{t,k}(t) \times w_t(t)]|^2 df \left(\frac{d_k}{d_i}\right)^2}{n.\int_{\Delta f_j} |FFT[h_i(t) \times w_i(t)]|^2 df}\right) \quad (3)$$

where n_j ($n_j \leqslant 9$) is the number of scanning points behind the barrier, $h_{(t,k)}(t)$ and $h_i(t)$ are the transmitted component at the kth position and the incident component of the free-field impulse response, respectively. $w_t(t)$ and $w_i(t)$ are the transmitted component time window and the incident reference free-field component time window, respectively. d_k is the geometrical divergence correction factor for the transmitted component at the kth position. d_i is the geometrical divergence correction factor for the reference free-field component. The single-number rating of sound insulation DL_{SI}, in decibels, is given by the following equation:

$$DL_{SI} = -10\log_{10}\left(\frac{\sum_{j=m}^{18} 10^{-0.1SI_j} \times 10^{0.1L_j}}{\sum_{j=m}^{18} 10^{0.1L_j}}\right) \quad (4)$$

2.1.2. Scale model measurements

A scale model measurements campaign is carried out with an adaptation of the CEN/TS 1793-5:2003 in situ standard to such reduced size problems. The use of scale models is dictated by the simplicity in setting-up different complex configurations. Measurements are carried out in a quasi-anechoic room (CSTB, Scale Model Centre, Grenoble, France). The ground is simulated by a rigid PVC plate, a tweeter loudspeaker is chosen as sound source, the acquisition is achieved with a Pulse system developed by Brüel&kJær. The sensors used here to represent point sources are half-inch Brüel&kJær 4133 microphones (Fig. 5). This approximation has already been validated by Premat el al. [12] (Figs. 6–11 in the publication). The authors showed good agreement between

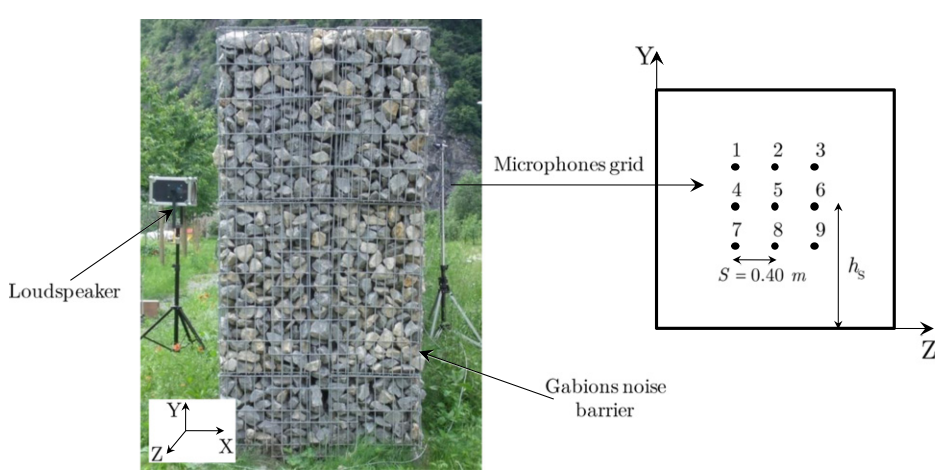

Fig. 4. Front view of the experimental device and measurement grid for sound insulation measurements.

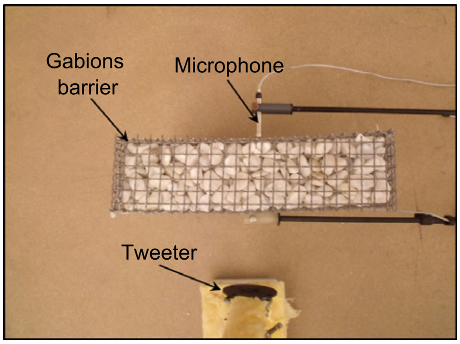

Fig. 5. Top view of the experimental set up for the scale model measurements (50 cm*40 cm*10 cm gabions noise barrier at model scale).

the excess attenuation results of scale model measurements performed with a half-inch microphone and those of BEM numerical simulations carried out with a point source for a wide frequency range.

Validation studies are carried out by comparing noise levels obtained using the scale model with those of the numerical calculations at a real scale. Measurements results have shown that reducing the size of the stones by 10 provides a great similarity below 2000 Hz at full scale (Fig. 6). Therefore, the scale factor chosen for the scale model measurements is 10. The dimensions and the distances of the CEN/TS 1793-5:2003 standard are divided by the scale factor and the same measurement techniques are chosen (impulsive method, temporal filtering, etc.). The granulometry of the stones used in the scale model is 0.7/1.5 cm. It has been measured using a gradation test with a nested column of sieves of different screen openings. The equivalent porosity ϕ of the gabions barrier is 40% for both numerical simulations and scale model measurements. For numerical simulations, ϕ is the ratio between the volume occupied by the stones and the total volume of the barrier. For scale model measurements, ϕ is determined by a simple method which consists in measuring the total volume V_t of a sample of stones filled with water and the volume of water V_w obtained after the removal of stones. The equivalent porosity ϕ is then the ratio between V_w and V_t.

2.1.3. Comparison and analysis

In this section the results of the in situ and scale model measurements as a function of the frequency are presented. The comparison between both approaches is carried out for the two tests in reflection and transmission according to the CEN/TS 1793-5:2003 standard. An Adrienne temporal filtering is applied on

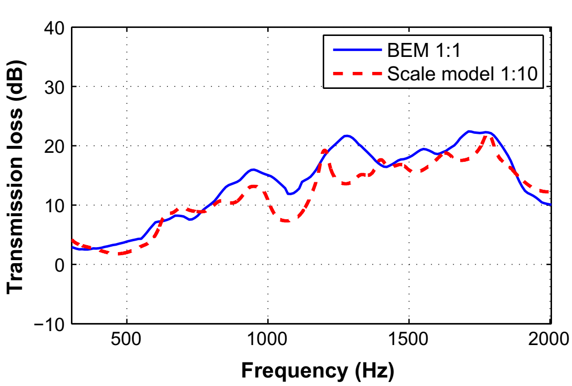

Fig. 6. Transmission loss of a gabions noise barrier as a function of frequency: comparison between scale model measurements (dashed line) and BEM simulations (solid line).

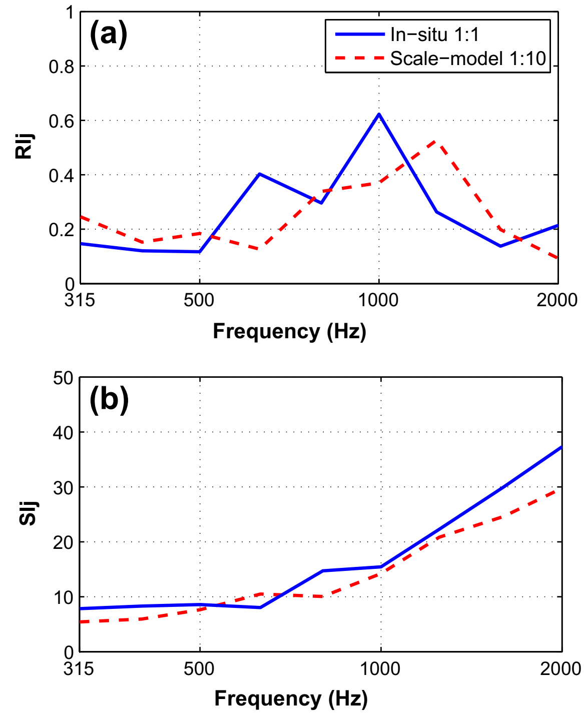

Fig. 7. Reflection index (a) and sound insulation index (b) as a function of frequency: comparison between in situ measurements (solid line) and scale model measurements (dashed line).

each of the components that we must extract from the impulse response. The low frequency limit f_{min} is inversely proportional to the width of the temporal window and depends on the dimensions of the noise barrier. For the tests in reflection and for angles of acquisition between $\theta = -40°$ and $\theta = 0°$ (see Fig. 2) the signal due to the reflection on the gabion and the one due to the reflection on the ground are very close in the time domain. For the tests in transmission the delay between the signal due to the transmission in the gabion and that due to the reflection on the ground for test points between 7 and 9 (see Fig. 4) and the delay between the signal due to the transmission in the gabion and that due to the diffraction by the edge, for test points between 1 and 3, are also very short. Therefore, the width of the temporal window has to be narrowed for some points of acquisition. The low frequency limit, in our case, is consequently about 250 Hz. The frequency results are therefore valid only above the 315 Hz one-third octave band.

The reflection and sound insulation properties of the gabions noise barrier are determined through the following two quantities: Reflection Index (RI) and Sound Insulation Index (SI). The variation of these two quantities as a function of frequency, for both types of measurement, is presented in Fig. 7. For RI curves, the agreement is acceptable. The single-number ratings of sound reflection are 4 dB and 5 dB for reduced and full scale measurements, respectively. The reflective performance of gabions noise barrier is average. For SI curves, there is good agreement between the results. For both measurements the transmission loss increases with increasing frequency and becomes an important factor in acoustic propagation when the wavelength approaches the size of the stones in the porous structure of the gabion. The single-number ratings of sound insulation are 19 dB and 20 dB for reduced and full scale measurements, respectively. These values show that the insulation performance of gabions noise barrier is average. In overall, the agreement is satisfactory between scale model and in situ measurements.

3. Evaluation of the acoustical effectiveness of low height gabions noise barriers

3.1. Numerical approach

3.1.1. The boundary element method

The boundary element method is a technique developed in the early sixties and is based on the integral equation theory [13,14]. This method appears more appropriate in an infinite space than the finite element method because only the surface of the domain boundary must be discretized. Its main advantage is that it allows any kind of shape and impedance condition values on the surfaces to be accounted for in a homogeneous atmosphere. The numerical code, MICADO [15], which we propose to use in this work is based on the direct integral equation formulation which can be expressed as:

$$p(M) = t(M) + \int_S p(Q)\left(\rho\omega^2 Y(Q)G(M,Q) - \frac{\partial G(M,Q)}{\partial n_Q}\right)dS(Q) \qquad (5)$$

In this equation the acoustic pressure p at any point M, for a source at any point Q, can be represented as the sum of a source term t and a radiated term. The radiated term is represented by an integral over the boundary S and is expressed in terms of the unknown pressure p, the Green function G and the admittance Y (ratio of velocity to pressure). The Green function describes the propagation of sound in the presence of an infinite ground and in the absence of diffracting objects. In this case, it is the sum of a direct term G_d, a reflected term G_r and a corrective term G_c which includes ground effects when the ground is not rigid [16].

$$\begin{aligned} G(M,Q) &= G_d(M,Q) + G_r(M,Q) + G_c(M,Q) \\ &= -\frac{i}{4}H_0(kr) - \frac{i}{4}H_0(kr^-) + P_\alpha(M,Q) \end{aligned} \qquad (6)$$

where r is the (M,Q) distance, r^- is the distance between M and the image of Q, H_0 is the Hankel function of the first kind and order zero and P_α is the correction factor for ground admittance.

The software MICADO uses a more complex approach based on a variational formalism where Eq. (5) is further developed and integrated a second time over S thus leading to a functional. The minimum of this functional also leads to a square symmetric matrix system. This approach provides a solution numerically more stable and the order of the singularities is reduced. Boundaries are meshed at each frequency automatically according to a criteria of minimum number of elements per wavelength and per segment, which greatly reduces computation times. The Hankel functions which appear in the elementary Green's terms are tabulated and interpolated when needed, which reduces the computation time required to compute the matrix by a factor of more than 20. The elementary integrations are done quite classically using Gauss integrations. In MICADO, the number of Gauss points NG may vary depending on the distance between points. Indeed, for short distances r (high values of $1/r$ terms) one will locally require a higher integration order. These aspects make MICADO a specially optimized software in calculation time.

In the numerical simulations of gabions noise barriers, the objects to be meshed are the stones. However the main problem in 3D simulations is still a high calculation time, especially when a large number of stones, that are very close to each other, is considered. Consequently, it was decided to carry out calculations with a 2D model. The calculation time depends also on some other parameters specially the number of frequencies per third octave band Nf and the number of Gauss points NG for the computation of elementary matrices. Preliminary calculations carried out to ensure convergence of numerical calculations are presented in Fig. 8.

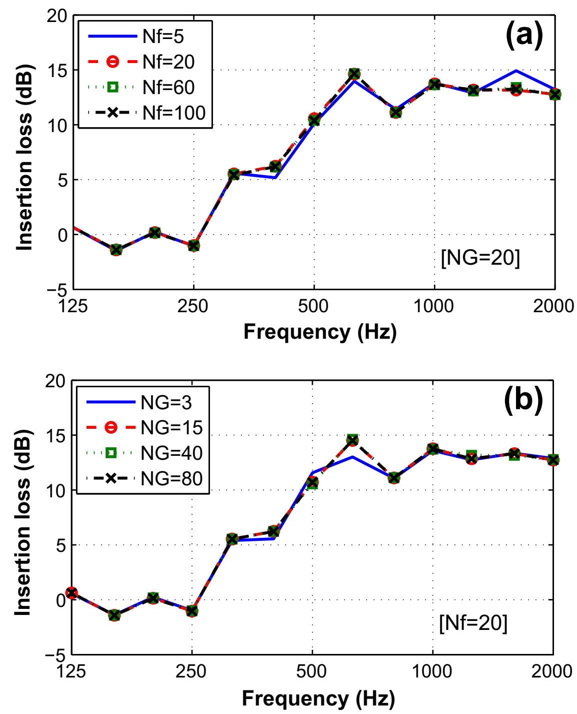

Fig. 8. Efficiency of gabions noise barrier: effect of the frequency resolution Nf (a) and the number of Gauss points NG (b) for convergence test.

20 frequencies per third octave band and 15 Gauss points are found to be sufficient for the convergence of the numerical results.

3.1.2. Simulations

In this section, the acoustic performance of low height gabions noise barriers along a two-lane road is studied as shown in Fig. 9. The width of each traffic lane is 4 m, both the street surface and pavement are modeled as rigid. Four sources are considered: two located at a height of 0.01 m (S2 and S4, representing light vehicle rolling noise) and two located 0.3 m above the road (S1 and S3, representing light vehicle engine noise). The point sources are located in the middle of the road lines. To estimate the global insertion loss in dB(A), the A-weighted road traffic noise spectra (for rolling and engine noises) calculated with weights according to the European Harmonoise model [17] are used.

The geometry of the problem is bi-dimensional: the source is an infinite linear coherent source and all the obstacles remain unchanged and infinite along a direction perpendicular to the vertical section plane. A homogenous atmosphere is assumed. Five noise barriers are considered in this numerical study. The reference case for all tests is a completely rigid barrier nb1. Four 1 m high and 1 m wide gabions barriers were tested with different properties (Fig. 10). For these barriers, the stones modeled with seven sided polygons are generated and positioned randomly. To avoid duplication, each stone is tested against the previous ones until there is no place left for stones filling. The numerical results will be presented for one instance of such a random generated geometry. Previous calculations had shown that this is adequate since the difference in global effectiveness between several realizations do not exceed 0.5 dB(A). Two granulometries of stones are used: g_1 = 15/20 cm and g_2 = 05/10 cm. The gabions barrier nb2 of granulometry g_1 and the barrier nb3 of granulometry g_2 are simple structures of gabions in which the stones are randomly distributed. The gabions barrier nb4 is a layered structure with two layers of small stones (granulometry g_2) on the ends and a middle layer of big stones (granulometry g_1). The gabions barrier nb5 is a layered structure

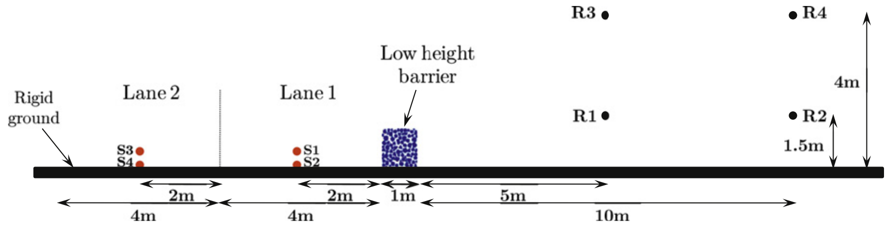

Fig. 9. Geometrical configuration.

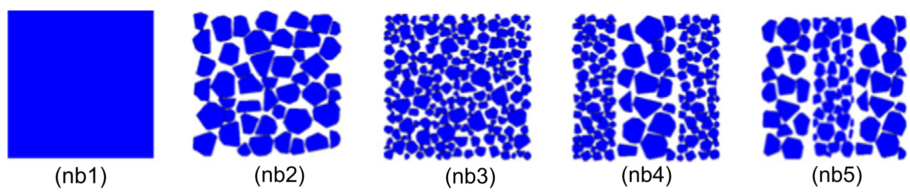

Fig. 10. Noise barriers studied: (nb1) rigid noise barrier, (nb2) and (nb3) classical gabions noise barriers, (nb4) and (nb5) layered structures of gabions noise barriers.

with two layers of big stones on the ends and a middle layer of small stones. For all gabions barriers, the stones are modeled by seven sided polygons; the porosity is around 40%, it corresponds to the real percentage of air in real noise gabions barriers.

Four receivers R1, R2, R3 and R4 are considered: R1 and R2 are representative of human ears: they are 1.5 m high and they are located 5 m and 10 m behind the gabion barrier, respectively. R3 and R4 are representative of the first floor of a building: they are 4 m high and they are located 5 m and 10 m behind the gabions protection, respectively.

3.1.3. Numerical results

Two types of results are presented here. First, the effectiveness of the four cases of noise barriers is given as a function of frequency. Second, the results of the global effectiveness in dB(A), using a road traffic noise spectrum, are detailed.

3.1.3.1. Effectiveness as a function of frequency. In this section the four cases of noise protections are considered and compared through their insertion loss spectra to a rigid barrier taken as the reference case. The barrier insertion loss is the difference of received sound pressure level between the situations without and with the barrier, for the same source–receiver configuration. It indicates the true noise barrier benefit at the receiver.

Calculations are carried out taking 20 equally-spaced frequencies per third octave band. Previous calculations have shown that this is adequate to ensure convergence of calculations. The insertion loss for each octave band is given by:

$$IL_{\Delta f} = 10\log_{10}\left(\left|\frac{P_{ref}(\Delta f)}{P_{nb}(\Delta f)}\right|^2\right) \tag{7}$$

where $P_{ref}(\Delta f)$ is the acoustic pressure for the reference configuration without the low height protection in the third octave band Δf and $P_{nb}(\Delta f)$ is the acoustic pressure for the configuration with the low height noise barrier in the third octave band Δf. The global source strength is obtained by summing the individual source energies (sources are considered incoherent with each other). The insertion loss spectra for all studied barriers and the four receivers are given in Fig. 11.

For receivers R1 and R2 which stand for pedestrians situated behind the barrier, the insertion loss spectra present two different behaviors as a function of frequency. The values of insertion loss of gabions protections, at medium and high frequencies, are very satisfactory and they are nearly equal to those of the rigid barrier: it seems that diffraction by the top edge of the noise barrier is the dominating factor at these frequencies. Values of the insertion loss range from 5.8 dB(A) up to 8.1 dB(A) when considering two vehicles in both lanes. Unlike the latter behavior, the performance of gabions barriers nb2, nb3, nb4 and nb5, compared to the reference rigid barrier, are slightly worse at low frequencies before the third octave band of 500 Hz. It should be noted that the gabions barriers nb2 and nb3 behave as a low pass filter with a cutoff frequency equal to 250 Hz. The degraded values of insertion loss at low frequencies are due to the acoustic transparency and the permeability of gabions which presents 40% of air in the mesoscopic scale. At medium frequencies the barrier nb2 is more effective than the barrier nb3. This is due to the large wavelength compared to the size of the stones of the barrier nb3. The layered structures nb4 and nb5 have been proposed in this research to improve the effectiveness of gabions barriers nb2 and nb3. As shown in Fig. 11, additional peaks of insertion loss and an increased shielding up to 4 dB at some low frequencies are observed. This is due to the change of impedance in the layered structures which affect the propagation of the acoustic wave inside the gabions barrier passing from one layer to another. On each interface between two layers of different properties (granulometry, density), a part of the acoustic energy is reflected when the sound velocity and the wavelength are changed.

For receivers R3 and R4, the difference between gabions and rigid protections effectiveness is not remarkable. A low insertion loss is obtained for the different noise barriers. The global insertion loss values range from 1.8 dB(A) up to 4.5 dB(A). This is due to the height of these receivers which are in a direct line of sight of the left sources. Indeed, low height barriers are essentially dedicated to abate noise for receivers of limited height (pedestrians and cyclists) and not for higher floors of buildings.

3.1.3.2. Global effectiveness in dB(A). The global insertion loss in dB(A) is given by the following formula:

$$IL_A = 10\log_{10}\left(\frac{\sum_{\Delta f}10^{(L_{WR}+EA_{ref,\Delta f})/10} + \sum_{\Delta f}10^{(L_{WP}+EA_{ref,\Delta f})/10}}{\sum_{\Delta f}10^{(L_{WR}+EA_{nb,\Delta f})/10} + \sum_{\Delta f}10^{(L_{WP}+EA_{nb,\Delta f})/10}}\right) \tag{8}$$

where $EA_{ref,\Delta f}$ is the excess attenuation calculated for the reference configuration without the noise barrier and for the third octave band Δf and $EA_{nb,\Delta f}$ is the excess attenuation calculated in the configuration with the noise barrier and for the third octave band Δf.

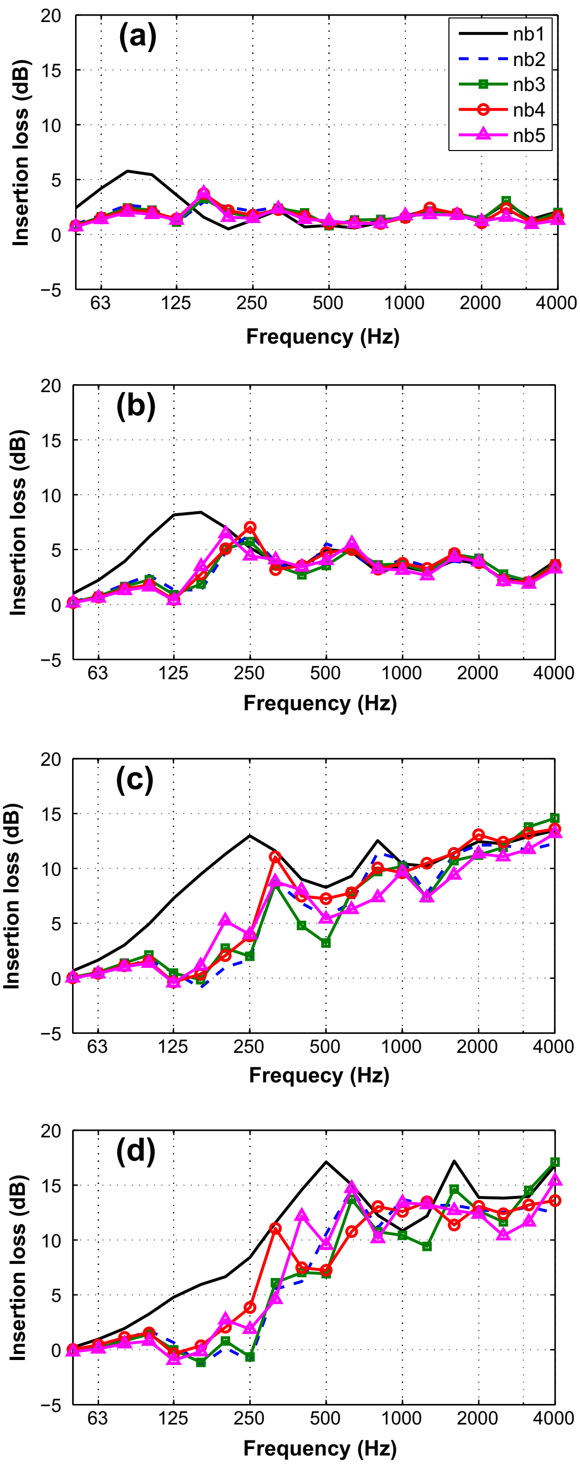

Fig. 11. Efficiency of the different noise barriers as a function of frequency for the four receiver positions. (a) R3 at d = 5 m and h = 4 m; (b) R4 at d = 10 m and h = 4 m; (c) R1 at d = 5 m and h = 1.5 m; (d) R2 at d = 10 m and h = 1.5 m.

Table 1
Insertion loss in dB(A) of the different noise barriers for the four receiver positions: vehicle speed is 30, 50, 70 km/h. L1 denotes traffic line 1, L2 denotes traffic line 2.

		1 Vehicle in L1			1 Vehicle in L2			2 Vehicles in L1 and L2		
		30 km/h	50 km/h	70 km/h	30 km/h	50 km/h	70 km/h	30 km/h	50 km/h	70 km/h
nb1	R1	9.6	10.2	10.8	7.6	8.5	8.9	8.6	9.6	10.1
	R2	10.1	10.9	11.2	7.7	8.0	8.2	9.1	9.8	10.3
	R3	4.1	4.1	4.1	0.1	0.0	0.1	2.1	1.9	1.9
	R4	8.5	8.6	8.7	2.0	1.5	1.3	4.5	4.0	4.0
nb2	R1	6.7	7.4	8.1	6.0	7.0	7.2	6.3	7.2	7.8
	R2	7.1	7.6	8.3	6.2	7.2	7.4	6.7	7.4	8.1
	R3	3.8	4.0	4.0	0.1	0.1	0.0	1.9	1.8	1.8
	R4	6.1	7.0	7.7	1.8	1.5	1.3	4.0	3.9	3.9
nb3	R1	6.2	7.0	7.8	5.8	6.7	7.0	6.1	7.0	7.5
	R2	6.7	7.2	8.0	6.0	6.8	7.1	6.3	7.1	7.8
	R3	3.8	4.0	4.0	0.1	0.1	0.0	1.9	1.8	1.8
	R4	6.0	6.9	7.5	1.6	1.4	1.3	3.8	3.8	3.7
nb4	R1	7.0	7.8	8.4	6.3	7.3	7.6	6.6	7.5	8.1
	R2	7.3	8.0	8.6	6.5	7.6	8.0	6.9	7.8	8.3
	R3	3.8	4.0	4.0	0.1	0.1	0.0	1.9	1.8	1.8
	R4	6.3	7.2	7.9	1.9	1.7	1.5	4.2	4.1	4.1
nb5	R1	6.9	7.7	8.2	6.2	7.3	7.5	6.6	7.4	8.0
	R2	7.2	7.9	8.5	6.5	7.5	7.9	6.8	7.7	8.3
	R3	3.8	4.0	4.0	0.1	0.1	0.0	1.9	1.8	1.8
	R4	6.4	7.1	7.8	1.8	1.6	1.6	4.2	4.1	4.0

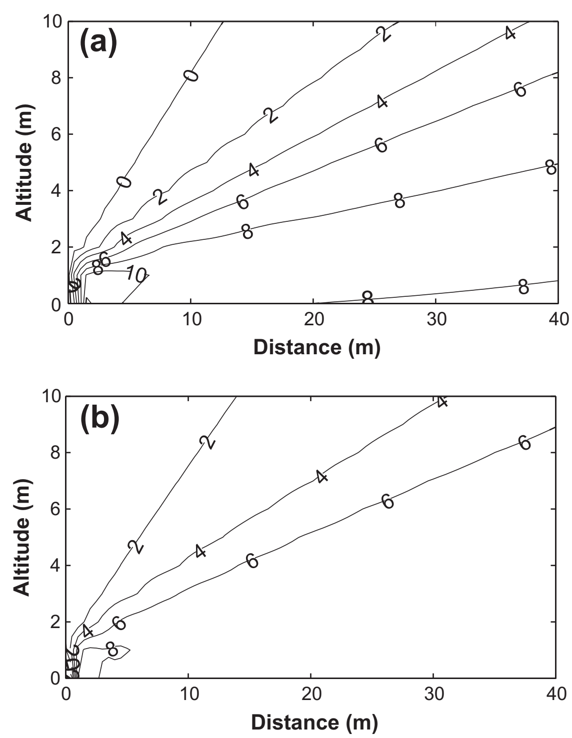

Fig. 12. Insertion loss in dB(A) for a large area. (a) Rigid barrier nb1; (b) gabions barrier nb2. Vehicle speed is 70 km/h.

L_{WR} and L_{WP} are the road traffic noise sound power levels in third octave bands due to rolling and propulsion noise, respectively.

The global traffic noise insertion loss values in dB(A), for the different noise barriers studied and for different vehicles speeds (30, 50, 70), are given in Table 1. Three traffic noise situations are considered: one vehicle in lane 1, one vehicle in lane 2, two vehicles in lanes 1 and 2. Lane choice has an influence on the effectiveness values, noise sources in lane 2 can contribute directly to the receivers of great height. Lane choice has a smaller effect for receivers R1 and R2 than for receivers R3 and R4. For the two last receivers, the global insertion loss values are nearly equal to zero when considering vehicles in lane 2 of the road. For receivers R1 and R2 and for all traffic noise situations, a larger insertion loss is observed with increasing vehicle speed when the rolling noise becomes more dominant. This effect is not observed for receivers R3 and R4 and a small decrease in the global insertion loss is

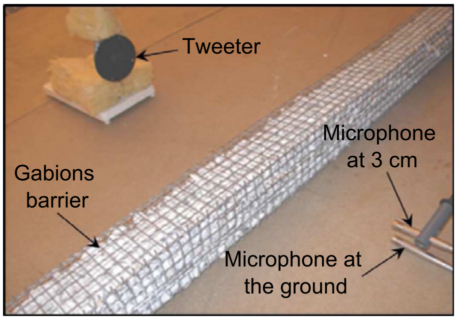

Fig. 13. Experimental set up for the scale model measurements of the effectiveness of low height gabions barrier.

mentioned when considering one vehicle in lane 2 or two vehicles in lanes 1 and 2. The global insertion loss values in dB(A) for the two protections nb4 and nb5 are close to those of the two protections nb2 and nb3. Indeed, the low frequencies have a low weight in the calculation of the global effectiveness due to the road traffic noise power level spectrum. To summarize, Table 1 shows, for receivers of limited height, significant values of global insertion loss of gabions noise barriers compared to those of the rigid reference case. The global insertion loss degradation do not exceed 2.5 dB(A) when vehicles are present in both road lanes.

In order to show the global insertion loss distribution behind the barrier, noise maps are given in Fig. 12: up to 40 m behind the noise barrier and up to a height of 10 m. A precision of four receivers per square meter is adequate to ensure the convergence of the results. The noise maps present the global effectiveness in dB(A) calculated with Eq. (8) using the Harmonoise road traffic model [17]. We present the results only for noise barriers nb1 and nb2 since the global insertion loss values of the other three barriers nb3, nb4 and nb5 are very close to those of the barrier nb2. Very satisfactory values of insertion loss are observed, for the two noise barriers, for receivers of limited height. Those results confirm the numerical results in dB presented with frequency spectra in Fig. 11.

3.2. Scale model measurements

Scale model measurements of the effectiveness of low height gabions noise barriers are carried out at a scale of 1:10 in order to confirm the results of the numerical simulations. The configuration used here is that shown in Fig. 9 except that we consider just two noise sources in lane 1. The photo presented in Fig. 13 shows the experimental set up for the scale model measurements. In this section, the granulometry of the stones is 1.1/1.7 cm for scale model measurements and 11/17 cm for numerical simulations. For the two methods, the equivalent porosity of the gabions barrier is 40% (determined as described above). In order to model road traffic sources close to the ground, we have used the reciprocity principle [18] which allows us to put the tweeter noise source in place of the microphone and vice versa. The noise sources S1 and S2 are presented by two microphones. The position and the height of the tweeter can be varied to present several point receivers.

The results of insertion loss as a function of frequency are shown in Fig. 14. They are compared with those of the numerical simulations using the BEM method. Globally, there is good agreement between measurements and numerical simulations. The insertion loss spectra present two different behaviors as a function of frequency. At low frequencies, values of measured insertion loss are slightly greater than those of numerical simulations. This is due to the bad response of the tweeter source at these frequencies. At medium and high frequencies, the opposite behavior is observed.

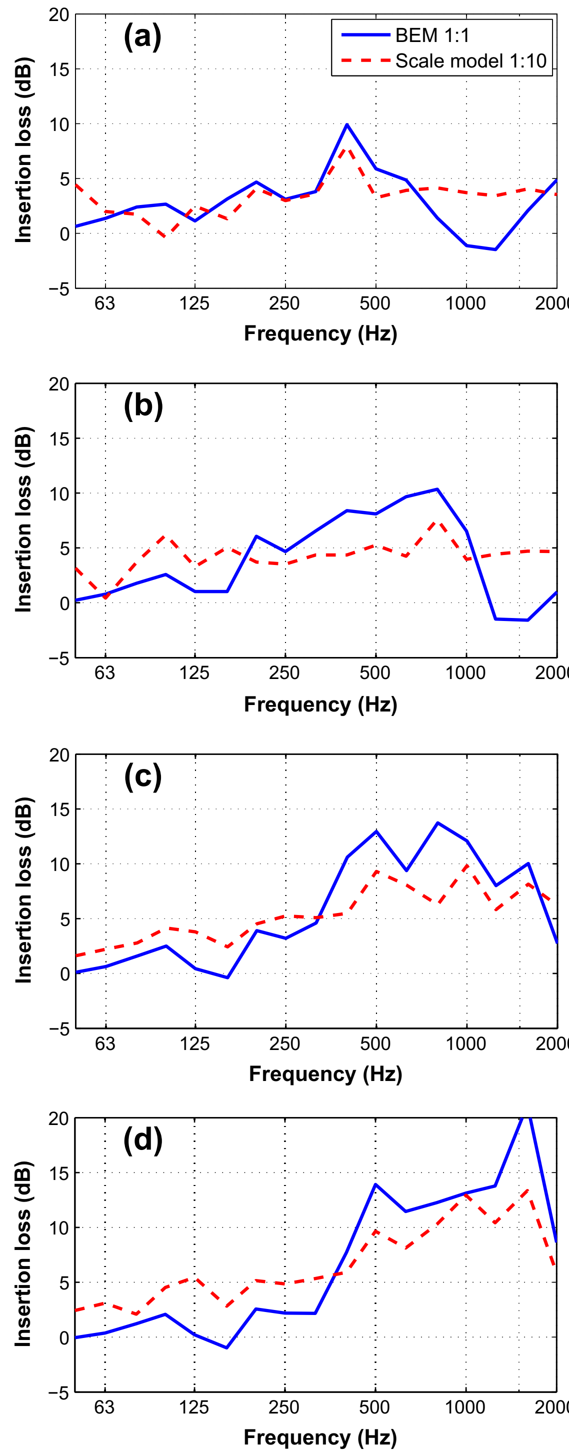

Fig. 14. Efficiency of low height gabions noise barrier as a function of frequency for the four receiver positions: BEM calculations (solid line), scale model measurement (dashed line). (a) R3 at $d = 0.5$ m and $h = 0.4$ m; (b) R4 at $d = 1$ m and $h = 0.4$ m; (c) R1 at $d = 0.5$ m and $h = 0.15$ m; (d) R2 at $d = 1$ m and $h = 0.15$ m. Distances and heights are at a scale 1:10.

This is due to the 2D simulations which do not take into account the energy that comes from all directions to the receiver point after penetration of the acoustic waves in the porous structure of the gabions barrier. The effectiveness of the gabions barrier is sensitive to the position of the receiver especially when the receivers are in a direct line of sight of the noise sources. This explains the low insertion loss values for the two receivers R3 and R4 located at a height

Table 2
Insertion loss in dB(A). Scale: scale model measurements; MICADO: theoretical BEM model simulations.

Receiver	ILA in dB(A)	
	Scale 1:10	MICADO 1:1
R1	6.0	6.4
R2	6.3	6.8
R3	2.9	3.2
R4	4.5	5.3

of 40 cm at model scale. Values of the global insertion loss in dB(A) are summarized in Table 2. The theoretical and experimental results are compared for the four receiver positions. The differences between BEM calculations (MICADO) and scale model measurements results are mostly less than 1 dB(A).

4. Conclusions

The concept of natural gabions noise barriers, inserted in urban areas as efficient solutions for reducing ground transportation noise, has shown some interesting results. In situ and Scale model measurements have been carried out to determine the intrinsic acoustic characteristics of gabions noise barrier according to the CEN/TS 1793-5:2003 standard. Globally, there is good agreement between the two measurement campaigns which showed that noise gabions protections are acoustically effective in reflection and transmission. The single number ratings of the reflection and insulation indices are around 5 dB and 20 dB, respectively. Numerical simulations carried out using a 2D Boundary Element Method (BEM) have shown a significant effectiveness, at medium and high frequencies, of 1 m high noise gabions barriers for receivers of limited height behind the barrier. Their insertion loss can reach 8 dB(A). Scale model measurements have been carried out in order to compare the results with BEM simulations. The results have shown good agreement. Our study shows that gabions barriers, which are originally used as retaining structures or hydraulic protections, can be used as effective noise barriers. In this case, their implementation and maintenance are very easy and there are wide choices of useful material of construction.

Acknowledgments

This research has been undertaken in the frame of the European Project Number 234306 'HOSANNA'. The authors thank the two anonymous reviewers for their helpful comments on this manuscript.

References

[1] European Standard CEN/TS 1793-5:2003. Road traffic noise reducing devices – test method for determining the acoustic performance – Part 5: Intrinsic characteristics – in situ values of sound reflection and airborne sound insulation.
[2] Anai K, Fujimoto K. Application of a genetic algorithm as the selection technique for optimal measures against road traffic noise in city areas. Prague: Internoise; 2004.
[3] Baulac M, Defrance J, Jean P, Margiocchi F, Poisson F. Noise impact of innovative barriers dedicated to freight trains in urban areas. Edinburgh: Euronoise; 2009.
[4] Baulac M, Defrance J, Jean P, Margiocchi F. Efficiency of noise protections in urban areas: predictions and scale model measurements. Acust Acta Acust 2006;92:530–9.
[5] Thorsson PJ. Optimisation of low-height noise barriers using the equivalent sources method. Acust Acta Acust 2000;86:811–20.
[6] Ding L, Van Renterghem T, Botteldooren D. Estimating the effect of semi-transparent traffic noise barrier using the UWVF method. Edinburgh: Euronoise; 2009.
[7] Martin SJ, Hothersall DC. Numerical modelling of median road traffic noise barriers. J Sound Vib 2002;251:671–81.
[8] Watts G, Morgan P. Measurement of airborne sound insulation of timber noise barriers: comparison of in situ method CEN/TS 1793-5 with laboratory method EN 1793-2. Appl Acoust 2007;68:421–36.
[9] Garai M, Guidorzi P. European methodology for testing the airborne sound insulation characteristics of noise barriers in situ: experimental verification and comparison with laboratory data. J Acoust Soc Am 2000;108:1054–67.
[10] Garai M, Guidorzi P. In situ measurements of the intrinsic characteristics of the acoustic barriers installed along a new high speed railway line. Noise Control Eng J 2008;56:342–55.
[11] European Standard EN 1793-3. Road traffic noise reducing devices – test method for determining the acoustic performance – Part 3: normalized traffic noise spectrum; 1997.
[12] Premat E, Defrance J, Mos A, Chartier H. Towards an experimental benchmark test cases database for the validation of numerical models for outdoor sound propagation. Acust Acta Acust 2003;89:992–7.
[13] Ciskowski RD, Brebbia CA. Boundary element methods in acoustics. London: Elsevier Applied Science; 1991.
[14] Kirkup S. The boundary element methods in acoustics. Integrated sound software; 2007.
[15] Jean P. A variational approach for the study of outdoor sound propagation and application to railway noise. J Sound Vib 1998;212:275–94.
[16] Hothersall DC, Chandler-Wilde SN, Hajmirzae MN. Efficiency of single noise barriers. J Sound Vib 1991;146:303–22.
[17] Jonasson H, Sandberg U, van Blokland G, Ejsmont J, Watts G, Luminari M. Source modelling of road vehicles. Deliverable 9 of the Harmonoise project. Technical report HAR11TR-041210-SP10; 2004.
[18] Josse R. Notions d'acoustiques á l'usage des architectes ingénieurs urbanistes. Paris: Eyrolles; 1977.